

# HIGH PERFORMANCE IODINE FREQUENCY REFERENCE FOR TESTS OF THE LISA LASER SYSTEM

Klaus Döringshoff, Katharina Möhle, Moritz Nagel, Evgeny V. Kovalchuk, Achim Peters

*Humboldt-Universität zu Berlin, Institut für Physik, AG QOM  
Hausvogteiplatz 5-7, 10117 Berlin, Germany  
Email: Klaus.Doeringshoff@physik.hu-berlin.de*

## ABSTRACT

Forthcoming space missions like the Laser Interferometer Space Antenna (LISA) or the Space-Time Asymmetry Research (STAR) project call for optical frequency references with high frequency stability better than  $10^{-14}$  at averaging times longer than 1000 s. Since Nd:YAG lasers are planned to be used on these missions, new interest has arisen in the frequency stabilization of Nd:YAG lasers to hyperfine transitions in molecular iodine. Iodine stabilized lasers offer an absolute optical frequency reference with high frequency stability and low sensitivity to temperature fluctuations and magnetic fields in relative simple setups. Here we present our iodine frequency standard using modulation transfer spectroscopy with a multi-pass iodine cell showing a frequency stability of  $1 \cdot 10^{-14}$  at 1 s averaging time.

## INTRODUCTION

Future space missions like the Laser Interferometer Space Antenna (LISA) [1] or the Space-Time Asymmetry Research (STAR) project [2, 3] will test fundamentals of space-time at unprecedented precision: LISA should for the first time detect and observe gravitational waves from astronomical sources with a sensitivity of  $10^{-21}$ , the STAR1 mission goal is to measure the constancy of the speed of light to  $10^{-17}$  and the Kennedy-Thorndike coefficient of the Mansouri-Sexl test theory to  $7 \cdot 10^{-10}$ .

These missions goals define high requirements on the frequency stability of the laser systems: the STAR mission requires a frequency stability better than  $10^{-14}$  at averaging times of 6000 s and LISA requires laser frequency noise lower than  $30 \text{ Hz}/\sqrt{\text{Hz}} \cdot \sqrt{1+(3 \text{ mHz/f})^4}$  between 0.1 mHz and 1 Hz. Nonplanar ring oscillator lasers (NPROs) are well suited for these missions since they feature high optical output power, superb intrinsic amplitude and frequency stability, and space qualified models already exist. However, to achieve the frequency stability requirements mentioned above, frequency stabilization to an external reference is still necessary. Hyperfine-resolved optical transitions in molecular iodine ( $^{127}\text{I}_2$ ), which can be addressed with a frequency doubled output of a NPRO laser at 1064 nm, are excellent candidates for this purpose. The narrow linewidth of the hyperfine components and a strong absorption coefficient at 532 nm allow for the realization of reliable and practical secondary frequency standards for space missions, as well as numerous terrestrial applications.

Several optical layouts have been proposed and realized for implementing highly stable iodine frequency standards at 532 nm. Most of them use modulation transfer spectroscopy (MTS) [4] and its modifications, but intra-cavity approaches are investigated as well [5]. The best current iodine references achieve a frequency stability of  $2.3 \cdot 10^{-14}$  at 1 s averaging time reaching  $4\text{-}5 \cdot 10^{-15}$  after 200 s [6, 7].

Here we present our iodine frequency reference for the validation of the stability and tuneability of optical frequency references that are developed in our group [8] for the space borne gravitational wave detector LISA. We have realized a modulation transfer spectroscopy setup with an 80 cm iodine cell in three fold pass configuration. We have investigated the frequency stability of this setup in comparison to a highly stable cavity made from an ultra low expansion (ULE) glass ceramic, finding a frequency stability of  $1 \cdot 10^{-14}$  between 1 s and 500 s of averaging time.

## EXPERIMENTAL SETUP

In our Laboratory we maintain a cross-linked system of optical frequency references including molecular standards based on methane and iodine, as well as several high-finesse optical cavities made of fused silica and ULE. In order to determine the performance of an individual reference, we compare its frequency stability to at least two other references.

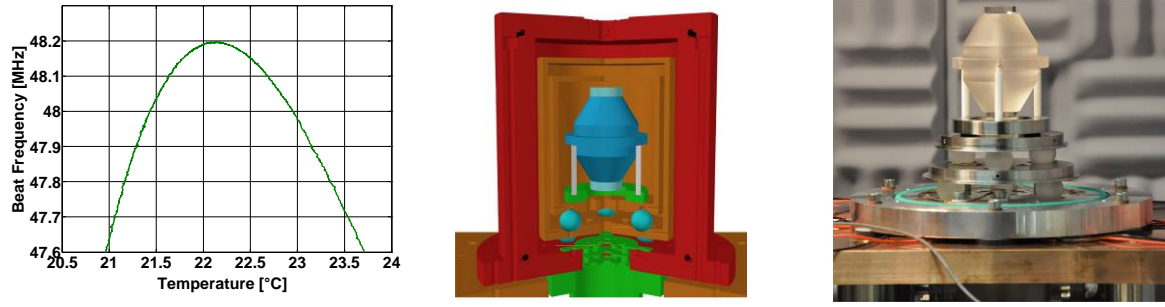


Fig. 1. (Left) Turning point of the coefficient of thermal expansion of the ULE resonator at 22°C, (middle) CAD sketch of the vacuum chamber, (right) photo of the ULE resonator and thermal shield base plates on glass balls with kinematical bed.

### ULE Resonator Setup

A NPRO laser (Lightwave LW124) is stabilized to a high performance ULE resonator using the Pound-Drever-Hall (PDH) stabilization technique. The ULE resonator consists of high finesse ULE mirrors attached to a vertically, midplane mounted 77.5 mm long tapered ULE spacer [9]. The resonator exhibits a finesse of 250000 and a cavity linewidth of 6 kHz. The turning point of the coefficient of thermal expansion (CTE) has been determined to 22.1 °C, see Fig. 1 (left). It is mounted in an aluminum vacuum chamber that is evacuated to  $1 \cdot 10^{-7}$  mbar using a 20 l ion pump and is temperature stabilized to the turning point of the CTE. The temperature fluctuations of the vacuum chamber are less than 30 mK in 60 h. Inside the vacuum chamber, the ULE resonator is enclosed by two thermal shields which rest on glass balls having low thermal conductivity in a kinematical bed thus providing excellent passive thermal isolation, Fig. 1 (middle and right). In order to determine the thermal isolation of this setup we placed a resonator made from aluminum inside the vacuum chamber. The temperature of the aluminum vacuum chamber was cycled and the response of the aluminum resonator was analyzed. A fit of a first order low pass to the measured transfer function revealed an effective time constant of  $10^8$  s.

The vacuum chamber and the PDH optics are mounted on a small optical breadboard (60 x 60 cm) which is placed on a passive vibration isolation table (MinusK 650BM-1), and the whole setup is surrounded by an acoustic isolation box. The light from the remote laser is fiber coupled to the setup and about 40  $\mu$ W of optical power are coupled into the resonator with a coupling efficiency of about 60 %. For the generation of the sidebands for PDH stabilization, instead of using an EOM, the laser crystal is modulated at a mechanical resonance of 444 kHz. The PDH error signal is generated using 3f demodulation to avoid problems associated with residual amplitude modulation (RAM) at 1f. With a power related frequency shift of about 4 Hz/ $\mu$ W, an intensity stabilization of the light coupled to the ULE resonator was found to be unnecessary.

In order to determine the frequency stability of the ULE resonator stabilized laser, its frequency was compared with other lasers that are stabilized to the iodine reference and a fused silica (FS) resonator that is used in a modern Michelson-Morely experiment [10]. The stabilized lasers are heterodyned on a fast photodiode and the beat note is analyzed. Since the beat note of the modulated lasers shows a complex spectrum, the carrier is filtered with a tracking oscillator and then counted using frequency counters (SR620, Pendulum CNT-90).

The beat note measurement with an iodine reference reveals a linear drift of the ULE resonator of -50 mHz/s that is ascribed to the isothermal creep of the ULE material. The beat note with the FS resonator stabilized laser exhibits a drift on the order 10 Hz/s dominated by the thermal drift of the (not actively temperature stabilized) fused silica resonator. The drift was subtracted by fitting a third order polynomial to the beat time record. From this data we calculate the relative Allan deviation and the frequency noise amplitude spectral density (ASD), shown in Fig. 2. Note that in the depicted figures, the data was divided by a factor of  $\sqrt{2}$  since both resonators have about equal thermal noise floors. The thermal noise floor of the ULE resonator and the FS resonator has been calculated to  $1.07 \cdot 10^{-15}$  and  $1.10 \cdot 10^{-15}$ , respectively, using formulas given in [11]. The ASD shows white frequency noise of 0.3 Hz/ $\sqrt{\text{Hz}}$  from 1 Hz to 500 Hz. A resonance peak at 2 Hz is caused by seismic fluctuations in the laboratory (situated on the eighth floor of the building). Further resonances at Fourier frequencies above 20 Hz are mainly caused by fiber noise (the light from the lasers is transferred to the setups via optical fibers without fiber noise cancellation). The ASD further indicates that the frequency stability of both resonators is close to the estimated thermal noise floors from 1 Hz down to 1 mHz. The Allan deviation shows minimum frequency instability of  $1.5 \cdot 10^{-15}$  at 1 s averaging time. The deviation from the noise floor can be assigned to the fused silica (FS) resonator. The FS resonator exhibits a much

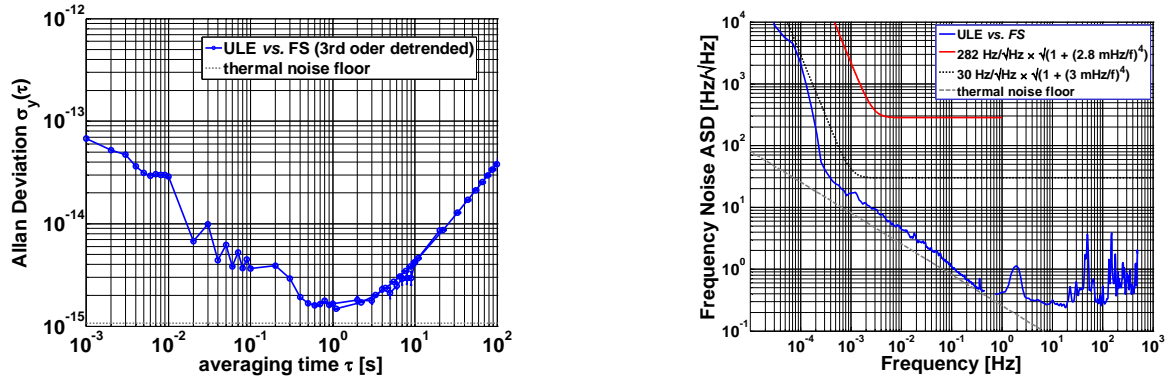


Fig. 2. ULE resonator frequency stability: (Left) Allan deviation of the beat note between two lasers stabilized to the ULE resonator and the fused silica resonator, (right) frequency noise ASD and initial and relaxed LISA requirements on laser system frequency noise [LISA-ASD-TN-5001, LISA-EST-SW-761]. In both graphs, the data was divided  $\sqrt{2}$ .

larger CTE than the ULE resonator and it is remarkable that the performance of the FS resonator is close to its thermal noise floor. This is due to the excellent passive thermal isolation provided the vacuum chamber, which is similar to the one containing the ULE resonator. In fact a thermal time constant of more than three month of the vacuum chamber was determined from the linear response of the FS cavity to a step function of the laboratory temperature (caused by a crash of the air conditioning unit).

### Iodine Frequency Reference Setup

The short term frequency stability of an iodine stabilization setup is mainly determined by the error signals slope-to-noise ratio. The noise is, in best case, determined by the detector shot noise while the slope depends on the linewidth of the interrogated transition and the signal strength. It is therefore beneficial for the performance of the iodine reference to have a long absorption length, which allows reducing the pressure in the iodine cell and thus reducing pressure broadening.

In our setup the laser source for the iodine standard is a frequency doubled Nd:YAG laser (Innolight Prometheus 50 NE) providing an optical output power of 90 mW at 532 nm. The molecular iodine is kept in an 80 cm long cell with anti-reflection coated windows. The cold finger of the iodine cell is temperature stabilized to  $-15^\circ\text{C}$ , corresponding to an iodine vapor pressure of 0.76 Pa.

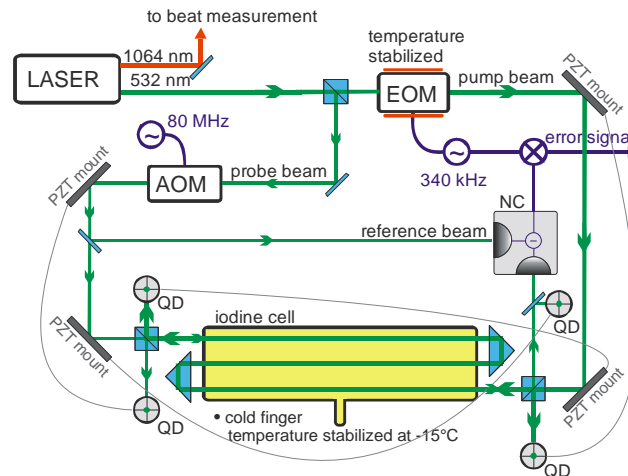


Fig.3. Schematic of the iodine frequency standard using an MTS setup with an 80 cm long absorption cell. A pointing stabilization is implemented to control the overlap of counter propagating beams inside the iodine cell. NC: noise canceling detector, QD: quadrant diode.

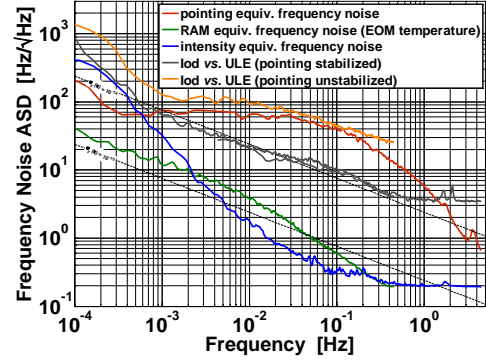
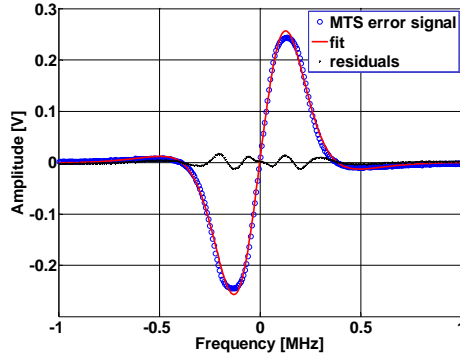


Fig. 4. (Left) MTS error signal generated at the DBM. The signal slope at line center is  $3 \mu\text{V}/\text{Hz}$ . The error signal was recorded by sweeping the LO frequency in the frequency range of  $\pm 1$  MHz at a rate of 0.01 Hz, (right) contribution of pointing noise, RAM and laser intensity noise to the laser frequency noise.

The modulation transfer spectroscopy (MTS) setup is shown in Fig. 3. The green output of the laser is split into a probe and a pump beam. The pump beam is phase modulated using an electro-optic phase modulator (EOM, Linos PM 25 KD\*P) by 340 kHz generated by a function generator (HP33120A). The EOM is temperature stabilized to about  $25^\circ\text{C}$  using a foil heater and a home made temperature controller with temperature fluctuations of 20 mK in 50 h. The pump beam diameter is then expanded to 3 mm and guided three times through the 80 cm long iodine cell by means of total internal reflection in right angle prisms, resulting in an absorption length of 2.4 m. The probe beam is frequency shifted by 80 MHz using an AOM in order to avoid interferences of the pump and probe beam. A fraction of the probe beam is split off for use in an intensity noise canceling detection scheme. The probe beam is then also expanded to a beam diameter of 3 mm and guided through the cell in opposite direction to the pump beam. The probe and pump beam power are set to about 7 mW and 17 mW, respectively. The probe beam is detected with an intensity noise canceling detector [12] that provides almost (3 dB above) shot noise limited detection even with the “noise eater” of the laser being disabled. The 340 kHz signal generated at the detector is band pass filtered, amplified and sent to a double balanced mixer. The rf signal is demodulated by mixing with a LO signal at the same frequency that is phase locked to the LO driving the EOM in order to generate the error signal.

In order to precisely characterize the MTS error signal, we offset phase locked the Prometheus laser and another laser, that was stabilized to the ULE resonator, to a local oscillator (SRS DS345). The LO frequency was chosen such that the Prometheus laser interrogated the  $a_{10}$  component of the transition R(56) 32-0 and then modulated at a low frequency. This way a clean record of the error signal is obtained. The recorded MTS error signal shown in Fig. 4 (left) exhibits a slope of  $3 \mu\text{V}/\text{Hz}$ . The detection noise measured at the IF port of DBM is on the order of  $10 \mu\text{V}/\sqrt{\text{Hz}}$ , thus giving an outstanding slope-to-noise ratio of the MTS error signal. By fitting a simple model to the recorded error signal we find relative large but symmetric residuals.

For frequency stabilization, the error signal is filtered by a proportional-integral controller and the laser frequency is controlled via a fast feedback channel to the laser piezo crystal actuator and a slow feedback channel to the laser crystal temperature. The control bandwidth of the frequency stabilization loop is typically about 40 kHz (determined from servo bumps).

Due to the long path through the iodine cell beam misalignment and beam pointing-jitter are a major source of frequency noise at Fourier frequencies below 10 Hz. This becomes clear by monitoring the stabilized laser frequency and the beam pointing using quadrant photo detectors. Depending on the beam overlap, a tilt of the final mirror before the iodine cell of  $1 \mu\text{rad}$  can cause a frequency shift on the order of 100 Hz. In order to improve the frequency stability of the iodine reference setup, a pointing stabilization of the pump and probe beam was implemented using quadrant photodiodes (OSI Optoelectronics QD50-0-SD) and piezo actuated mirror mounts (Thorlabs KC1-T-PZ) as shown in Fig. 3. Due to mechanical resonances of the mirror mounts at few hundred Hz the control bandwidth of the feedback loop was limited to 100 Hz, which is sufficient to control the relevant pointing noise. Fig. 4 (right) shows the frequency stability of the iodine reference with the pointing stabilization enabled and disabled. It is visible, that the frequency stability is improved when the pointing stabilization is enabled. However, the performance seems to be still limited by residual pointing noise which is indicated by out of loop measurements of the pointing noise.

The contribution of intensity noise and RAM has been investigated as well. The estimated equivalent frequency noise due to laser intensity noise, RAM and pointing is shown in Fig. 4 (right). The influence of laser intensity noise and RAM seem to not limit the frequency stability at Fourier frequencies above 1 mHz.

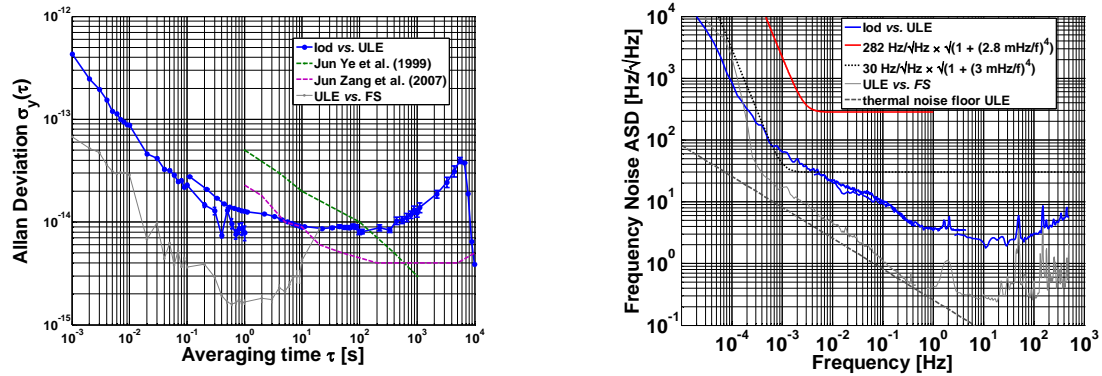


Fig. 5. Iodine standard frequency stability: (left) Allan deviation in comparison to other iodine standards [6, 7], (right) corresponding ASD along with to the initial and relaxed LISA requirements on the laser system. The performance of the ULE reference is shown for comparison.

## Frequency Stability

A fraction of the infra red (IR) output of the stabilized laser is used for beat note measurements. The performance of the iodine frequency standard was determined with respect to a laser locked to the ULE resonator. The Allan deviation and the ASD were calculated and are shown in Fig. 5. The linear drift of the ULE resonator was subtracted. Due to the long absorption length the measurements show good short term stability. The ASD shows white frequency noise below 4 Hz/ $\sqrt{\text{Hz}}$  from 500 mHz to 100 Hz in agreement with the slope-to-noise ratio. The frequency noise at Fourier frequencies below 500 mHz can be assigned to residual pointing noise that is not sufficiently suppressed by the pointing stabilization. This has to be improved for better performance of the long term stability of the iodine reference. A short term stability of  $8 \cdot 10^{-15}$  at 1 s averaging time has been determined from a data record of 10 s. The long term stability shows a flicker floor around  $1 \cdot 10^{-14}$  at averaging times from 1 s to 500 s with a minimum of  $8 \cdot 10^{-15}$  at 100 s.

It is worth to mention, that the implementation of the intensity noise canceling detection scheme and the three-fold pass through the iodine cell have led to an improvement of the short term stability of the present iodine standard of about two orders of magnitude with respect to the precursor setup investigated previously [13].

## CONCLUSION

We stabilized a NPRO laser to the  $a_{10}$  component of the transition R(56) 32-0 of molecular iodine ( $^{127}\text{I}_2$ ) by means of an MTS setup featuring a threefold pass through an iodine cell and a pointing stabilization system. The frequency stability of this system was determined in comparison to another NPRO laser stabilized to a high performance ULE resonator. The measurements reveal a promising short term stability of  $1 \cdot 10^{-14}$  at 1 s averaging time and a flicker floor of about  $1 \cdot 10^{-14}$  from 1 s to 500 s. In order to further improve the performance of this iodine standard the pointing stabilization will be improved with respect to its long term stability. For ultimate performance the setup of a Zerodur bonded setup is considered.

## REFERENCES

- [1] K. Danzmann, "LISA mission overview," Adv. Space Res., vol. 25, pp. 1129-1136, 2000
- [2] S. P. Worden, "Technology Development for Fundamental Physics on Small Satellites", 37th COSPAR Scientific Assembly. Held 13-20 July 2008, in Montréal, Canada, p.2764
- [3] T. Schuldt et al. "The Space-Time Asymmetry Research (STAR) Program," within these proceedings
- [4] J. H. Shirley, "Modulation transfer processes in optical heterodyne saturation spectroscopy," Opt. Lett., vol. 7, pp. 537-539, November 1982
- [5] L.-S. Ma, J. L. Hall, "Optical Heterodyne Spectroscopy Enhanced by an External Optical Cavity: Towards Improved Working Standards," IEEE Quantum Electronics, vol. 26, pp. 2006-2012, November 1990
- [6] E. J. Zang, J. P. Cao, Y. Li, C. Y. Li, Y. K. Deng, and C. Q. Gao, "Realization of Four-Pass I2 Absorption Cell in 532-nm Optical Frequency Standard," IEEE Transactions on Instrumentation and Measurement, vol. 56, pp. 673-676, April 2007
- [7] J. Ye, L. Robertsson, S. Picard, L.-S. Ma and J. L. Hall, "Absolute frequency atlas of molecular  $\text{I}_2$  lines at 532 nm," IEEE Transactions on Instrumentation, vol. 48, pp. 544-549, April 1999

- [8] K. Möhle, K. Döringshoff, M. Nagel, E. V. Kovalchuk and A. Peters, "Piezo-Tunable High Finesse Cavity," within these proceedings
- [9] M. Notcutt, L.-S. Ma, J. Ye, and J. L. Hall, "Simple and compact 1-Hz laser system via an improved mounting configuration of a reference cavity," *Opt. Lett.*, vol. 30, no. 14, pp1815-1817, July 2005
- [10] S. Herrmann, A. Senger, K. Möhle, M. Nagel, E. V. Kovalchuk, and A. Peters, "Rotating optical cavity experiment testing Lorentz invariance at the  $10^{-17}$  level", *Phys. Rev. D*, vol. 80, 105011, November 2009
- [11] K. Numata, A. Kemery and J. Camp, "Thermal-Noise Limit in the Frequency Stabilization of Lasers with Rigid Cavities," *Phys. Rev. Lett.*, vol. 93, p. 250602, December 2004
- [12] P. C. D. Hobbs, "Ultrasensitive laser measurements without tears," *Appl. Opt.*, vol. 36, pp. 903-920, February 1997
- [13] E. V. Kovalchuk, T. Schuldt, A. Peters, "Combination of a continuous-wave optical parametric oscillator and a femtosecond frequency comb for optical frequency metrology," *Opt. Lett.*, Vol. 30, pp. 3141-3143, December 2005